

14p  
N63 22353

CODE-1

CHARGED PARTICLE RADIATION DAMAGE IN SEMICONDUCTORS, VIII:

THE ELECTRON ENERGY DEPENDENCE OF RADIATION  
DAMAGE IN PHOTOVOLTAIC DEVICES

(NASA CR 51530;

MR-33  
15 JULY 1963

8653-8025-KU-000} OTS:

\$2.60 ph, \$0.98 mf

[8]

(NASA Contract No. NAS5-1851)

NATIONAL AERONAUTICS AND SPACE ADMINISTRATION

GODDARD SPACE FLIGHT CENTER

OTS PRICE

XEROX \$ 2.60 ph  
MICROFILM \$ 0.98 mf



SPACE TECHNOLOGY LABORATORIES, INC.  
a subsidiary of Thompson Ramo Wooldridge Inc.  
ONE SPACE PARK • REDONDO BEACH, CALIFORNIA

Reproduced by  
NATIONAL TECHNICAL  
INFORMATION SERVICE  
Springfield, Va. 22151

CHARGED PARTICLE RADIATION DAMAGE IN SEMICONDUCTORS, VIII:  
THE ELECTRON ENERGY DEPENDENCE OF RADIATION DAMAGE IN PHOTOVOLTAIC DEVICES

by

↓  
J. M. Denney  
R. G. Downing

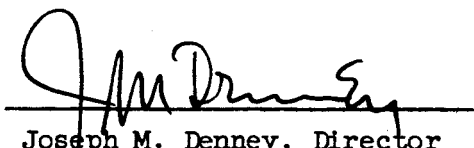
MR-33  
15 July 1963 26p 6 refs

8653-6025-KU-000

(NASA Contract No. NAS5-1851)

Solid State Physics Laboratory

Approved:

  
Joseph M. Denney, Director  
Solid State Physics Laboratory

8195109

SPACE TECHNOLOGY LABORATORIES, INC.,  
One Space Park  
Redondo Beach, California

ABSTRACT

22353

A series of experiments using electrons from 1 Mev to 40 Mev were performed to measure the energy dependence of electron radiation damage in p on n and n on p silicon and gallium arsenide solar cells. The experimental results indicate that: (a) 1 ohm-cm p on n silicon and gallium arsenide solar cells respond according to predicted energy dependence relationships based on simple displacement theory and (b) 1 ohm-cm and 10 ohm-cm n on p silicon solar cells depart from the simple theoretical predictions by exhibiting a much greater sensitivity to incident electron energy. The details of the mechanism responsible for the departure of p-type silicon from simple displacement theory are not clear at this time.

AUTHOR

ACKNOWLEDGEMENT

We are grateful to R. Jurgovan, H. Smith, and the electron linear accelerator staff of General Atomic, San Diego, for their assistance in the performance of this energy dependence experiment. The research and analysis were supported by the National Aeronautics and Space Administration, Goddard Space Flight Center, Greenbelt, Maryland.

TABLE OF CONTENTS

	<u>Page</u>
I. INTRODUCTION. . . . .	1
II. DESCRIPTION OF EXPERIMENTS. . . . .	1
Solar Cell Specimens. . . . .	2
Solar Cell Measurements . . . . .	2
Dosimetry . . . . .	3
Experimental Techniques . . . . .	5
III. EXPERIMENTAL RESULTS. . . . .	6
IV. SUMMARY AND CONCLUSIONS . . . . .	18
REFERENCES. . . . .	20

LIST OF ILLUSTRATIONS

<u>Figure</u>		<u>Page</u>
1	Solar Cell Short Circuit Current Degradation Under 3.0 Mev Electron Bombardment. . . . .	7
2	Solar Cell Short Circuit Current Degradation Under 5.2 Mev Electron Bombardment . . . . .	8
3	Solar Cell Short Circuit Current Degradation Under 7.9 Mev Electron Bombardment . . . . .	9
4	Solar Cell Short Circuit Current Degradation Under 8.5 Mev Electron Bombardment . . . . .	10
5	Solar Cell Short Circuit Current Degradation Under 18.5 Mev Electron Bombardment . . . . .	11
6	Solar Cell Short Circuit Current Degradation Under 21.2 Mev Electron Bombardment . . . . .	12
7	Solar Cell Short Circuit Current Degradation Under 40 Mev Electron Bombardment . . . . .	13
8	Critical Flux Determination of Electron Damage Energy Dependence . . . . .	16
9	K Value Determination of Electron Damage Energy Dependence. . .	17

## I. INTRODUCTION

The degradation under 1 Mev electron bombardment of the electrical characteristics of silicon solar cells in the conversion of light energy to electrical power has been extensively studied<sup>1,2</sup>. Because of the importance of electrons in the energy range from 1 to 10 Mev in the artificial radiation belt, an initial experiment<sup>3</sup> was conducted in February of 1963 to compare the observed electron energy dependence with energy dependence relationships based on simple displacement theory and classical Rutherford scattering. This experiment, conducted at the General Atomic linear electron accelerator facilities in San Diego, indicated that although p on n silicon solar cells agreed with the theoretical predictions, n on p silicon solar cells exhibited a much higher energy dependence than predicted. To determine the significance of the steeper energy dependence of n on p cells, the two observed energy dependences were integrated with the fission electron energy spectrum and normalized to equivalent 1 Mev electrons. The result of this calculation was that the degradation rate of n on p silicon solar cells under fission electron energy spectrum bombardment would be approximately a factor of three faster than predicted by the theoretical energy dependence.

Because of the importance of the more radiation resistant n on p cells in the construction of satellite solar cell power supplies, a second series of experiments were performed in March, 1963 at the General Atomic linear electron accelerator facilities. The objectives of this second experiment were to obtain more accurate quantitative data on the energy dependence of electron radiation damage and to expand the scope of the results in both type of device and energy range. The purpose of this report is the presentation of the electron radiation damage data on photovoltaic devices and the dependence on electron energy from these later experiments.

## II. DESCRIPTION OF EXPERIMENTS

The primary objective was the acquisition of quantitative experimental data on the energy dependence of electron radiation damage in silicon and gallium arsenide solar cells. Since a previous experiment<sup>3</sup> had shown that abnormal responses were exhibited by n on p silicon solar cells, a good deal of effort

was expended to insure quantitative accuracy of both dosimetry and solar cell measurements. The remainder of this section is devoted to detailed descriptions of the test specimens themselves, the measurements performed on the test specimens, the dosimetry measurements of beam energy, intensity, and distribution, and the general experimental techniques of the experiment.

### Solar Cell Specimens

The test specimens consisted of both silicon and gallium arsenide solar cells and additional silicon slabs for energy level determinations through Hall measurements. The solar cells consisted of commercially available Hoffman 1 ohm-cm p on n silicon solar cells, Western Electric 1 ohm-cm n on p silicon solar cells, Hoffman 10 ohm-cm n on p silicon solar cells, and RCA p on n gallium arsenide solar cells. These particular solar cells were chosen because of the large amount of data existing on these types, their established quality and reproducibility, and their representation of state-of-the-art devices currently available. The cells chosen for this experiment were preselected through short circuit current, diffusion length, and spectral response measurements and were, therefore, as closely matched and representative of their type as possible.

The Hall specimens consisted of both p and n-type silicon with resistivities of 1 and 100 ohm-cm. The Hall specimens were precut to the conventional six-arm cross configuration for post-irradiation measurements of the Hall effect.

### Solar Cell Measurements

The measurements performed on the test solar cells at the linac site consisted of I-V characteristics under the STL light table using 2800°K unfiltered tungsten illumination. The illumination level was maintained at the same setting used in all previous experiments, i.e., 110 mw/cm<sup>2</sup> nominal sunlight equivalent. These I-V characteristics were used to obtain post-irradiation minority carrier diffusion length values under approximately one sun conditions. This diffusion length measurement technique, described in detail in a previous report<sup>4</sup>, consists of relating the observed short circuit current to a minority carrier diffusion length through an empirical relationship previously established under



1 Mev electron bombardment. All these measurements were obtained on each specimen before and after each successive irradiation. Additional diffusion length and short circuit current data were obtained after returning to STL to establish calibrations, short term annealing characteristics, and linearity of diffusion length with injection level. These data were utilized to establish K values and  $\phi_c$  values for determination of the energy dependences of the damage rates.

### Dosimetry

In order to obtain as accurate dosimetry as possible, particular attention was given to measurements of beam energy, distribution, and intensity. The electron beam energy was determined by General Atomic personnel with a calibrated steering magnet. This magnet had been previously calibrated through a series of range energy relationships to within  $\pm 2$  per cent. Magnet current was supplied by a regulated power supply insuring a constant magnetic field through the steering magnet. One of the primary causes of electron beam energy shift was inherent drift of the three linac Klystrons. Under the conditions of low beam current required for these experiments, considerable Klystron drift was observed during several series of experiments. The geometry of the accelerator and the particular beam port utilized in these experiments was such that several bends in the beam were required to bring the beam out of the experiment port. Since each of these bends requires an individual steering magnet, any appreciable drift or change in beam energy would result in complete loss of the beam at the port where the experimental apparatus was located. Consideration of all these factors, i.e., accuracy of beam energy determinations, Klystron drift, and accelerator geometry, results in a net estimated accuracy of beam energy measurements of  $\pm 2$  per cent at each experiment energy value. Additional corrections were applied for energy loss of the beam in traversing the exit port window and air before impinging upon the test specimens.

Beam spreading was accomplished with several quadripole defocusing magnets and air scattering to produce a large beam spot. Polaroid film was used to determine the beam position and distribution over the beam spot area and to position the experimental targets. The quadripole magnets were driven with regulated supplies and found to be quite stable. Due to the small diameter of the accelerator

drift tubes, however, a practical limit of the beam spot that could be produced before the beam struck the inside walls of the drift tubes was found. To obtain further defocusing, the experimental apparatus was located away from the beam port to take advantage of small angle air scattering for further improvement in beam size and distribution. The particular distance between the experimental apparatus and the beam exit port window was determined by the energy of the experiment. Polaroid film was used to obtain beam profiles and to position the experimental apparatus with respect to the center line of the electron beam. In all of the experiments, the total beam area exceeded  $10 \text{ cm}^2$  and usually was of the order of  $15 \text{ cm}^2$ . Only the center  $4 \text{ cm}^2$  of the total beam was used for sample irradiation insuring a uniform distribution across the test specimens.

Total beam current was monitored with a Faraday cup of conventional design. An inner, or sensing, chamber constructed of copper of sufficient thickness to stop 50 Mev electrons was mounted in a larger evacuated chamber which was pumped and trapped to a pressure of less than 1 micron. The bottom, or target area, of the Faraday cup contained an aluminum plate to reduce the back scattered electron component to a minimum. In addition, a copper back scatter shield was utilized to reduce the solid angle through which back scattered electrons could leave the chamber through the entrance aperture. Additional back scatter control was exercised through the application of grid bias directly above the entrance aperture to the inner sensing chamber. Application of grid voltage from -400 to +400 volts indicated that the back scattered component had been reduced to less than 5 per cent and, further, that the forward scattering from the 5 mil aluminum vacuum window of the Faraday cup was less than 2 per cent. A conservative estimate of the accuracy of the Faraday cup considering these factors is an accuracy of better than  $\pm 10$  per cent with a more probable realistic accuracy of  $\pm 5$  per cent. Subsequent comparisons of beam current with apparatus utilized by General Atomic personnel were in agreement to within 5 per cent. The output of the Faraday cup was fed directly to an integrating amplifier which measured both current and integrated charge to an accuracy of 1 per cent. This particular instrument is specifically designed to accept Faraday cup inputs and contains an input impedance of essentially zero ohms utilizing operational amplifiers.

### Experimental Techniques

The test specimens were mounted two at a time on aluminum plates. Each plate contained two identical types of cells. These plates were placed one at a time in a jig directly in front of the Faraday cup and integrated flux measurements were obtained simultaneously with the irradiation of the test specimens. Each group of two specimens was exposed to a predetermined integrated flux and removed for post-irradiation measurements. Following these measurements, additional irradiations were performed followed by further post-irradiation measurements on the same specimens. When a sufficient number of irradiations had been performed to define a straight line function of the degradation of short circuit current with the logarithm of the integrated flux, the specimens were removed and stored for later post-irradiation measurements at STL. Since a minimum of three different types of cells were tested at each energy, the irradiations were performed in an alternating sequence to remove any effect of machine and, hence, radiation environment shift on the experimental results. In addition, since each individual group of two specimens was always placed in exactly the same position in the beam, any nonuniformity or shift in electron flux distribution would produce a constant and, hence, observable difference. Since no systematic difference in experimental results due to position of the cells occurred, the beam uniformity was demonstrated.

Beam alignment and distribution were continuously checked throughout each series of experiments at a given energy with Polaroid film. In addition, beam energy measurements were performed utilizing the calibrated steering magnet before and after each series of runs and the deviation of beam energy from start to finish of a series of experiments was acquired. If the beam energy shift from start to finish of an experiment on a particular group of cells was found to be excessive, i.e., greater than 3 per cent, a second group of specimens was exposed in a repeat of the series of experiments at that energy to insure maximum accuracy in the determination of the energy dependence of the degradation rates.

### III. EXPERIMENTAL RESULTS

Separate linac experiments were conducted at seven energies: 3.0 Mev, 5.2 Mev, 7.9 Mev, 8.5 Mev, 18.5 Mev, 21.2 Mev, and 40 Mev. Included with these data in the experimental results are additional 1 Mev data acquired using the STL Van de Graaff. One ohm-cm p on n and 10 ohm-cm n on p silicon solar cells were irradiated at all of these energies. Additional data were acquired on 1 ohm-cm n on p silicon and p on n gallium arsenide solar cells at 1.0 Mev, 3.0 Mev, 7.9 Mev, and 40 Mev. The resulting energy dependence of the electron damage characteristic was determined by utilizing both K values and reciprocal critical fluxes. The K values were obtained from diffusion lengths measured with the Van de Graaff and with the calibrated light source. The reciprocal flux determinations were acquired from short circuit current degradation characteristics.

The observed degradation in I-V characteristics as a function of integrated flux for all of these specimens utilized in this experiment was consistent with previously reported data. These I-V characteristics were obtained with 2800°K unfiltered tungsten illumination at a sunlight equivalent intensity of 110 mw/cm<sup>2</sup> for a nominal 100 micron cell. Short circuit current densities were taken from these I-V characteristics and plotted as a function of integrated flux to determine the damage characteristics. These short circuit current degradation curves are shown in Figures 1 through 7 for each energy at which meaningful data were obtained. All of these data are shown as short circuit current density plots with the exception of the gallium arsenide data for which the absolute short circuit current for a 1 x 2 cm<sup>2</sup> cell is plotted directly for convenience in maintaining scale factors. Linear slopes of 6-1/4 ma/cm<sup>2</sup>-decade are fit to each group of data points. Critical fluxes are determined by observing the flux required to produce 19 ma/cm<sup>2</sup> on the 6-1/4 ma/cm<sup>2</sup>-decade slope. This critical flux is consistent with the critical fluxes described in all of our previous reports.

A short circuit current density of 19 ma/cm<sup>2</sup> is equivalent to 25 per cent degradation in short circuit current under 110 mw/cm<sup>2</sup> tungsten illumination for a nominal silicon solar cell having an initial minority carrier diffusion length of 100 microns. Since current state-of-the-art devices have longer

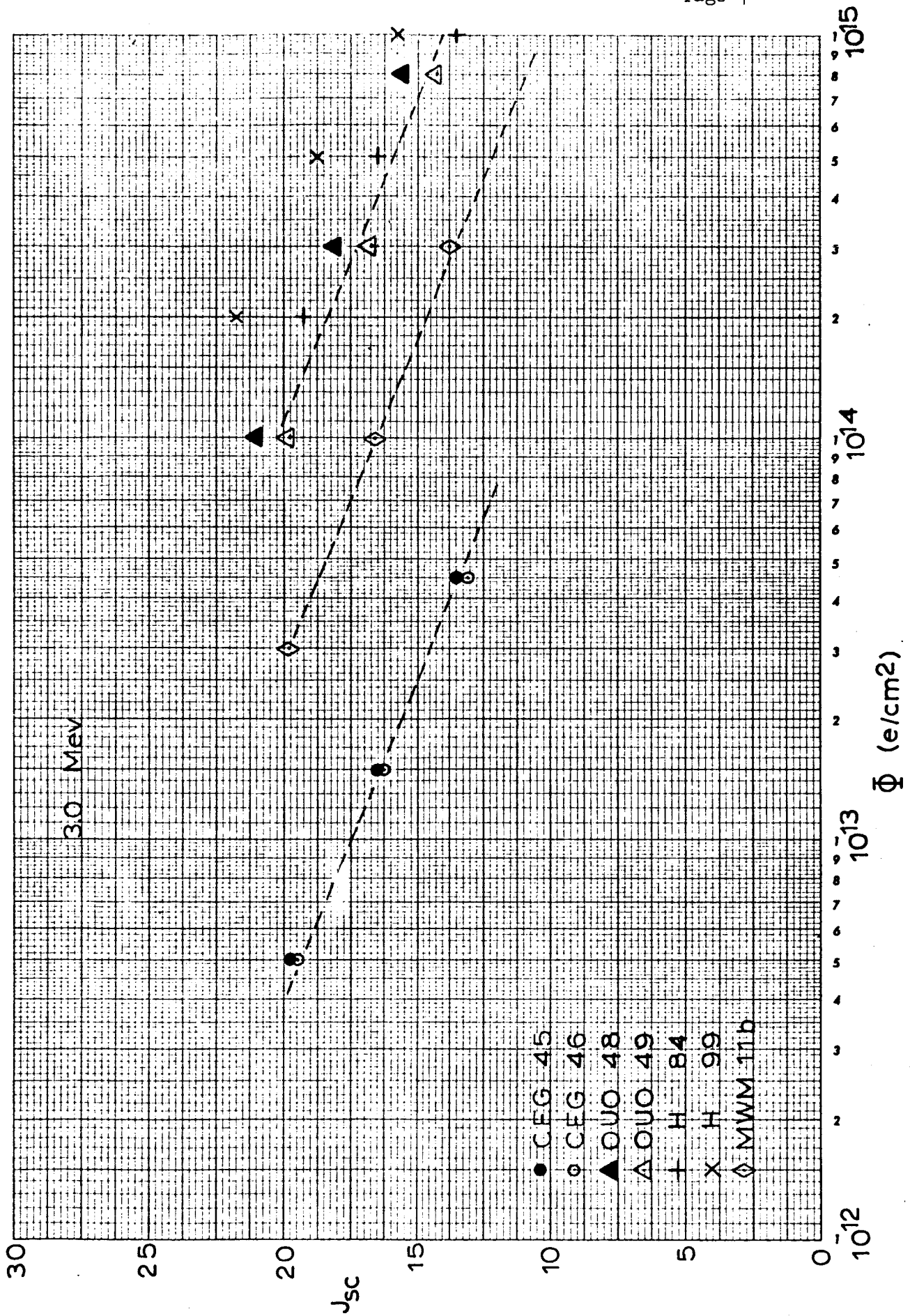


Figure 1. Solar Cell Short Circuit Current Degradation Under 3.0 Mev Electron Bombardment

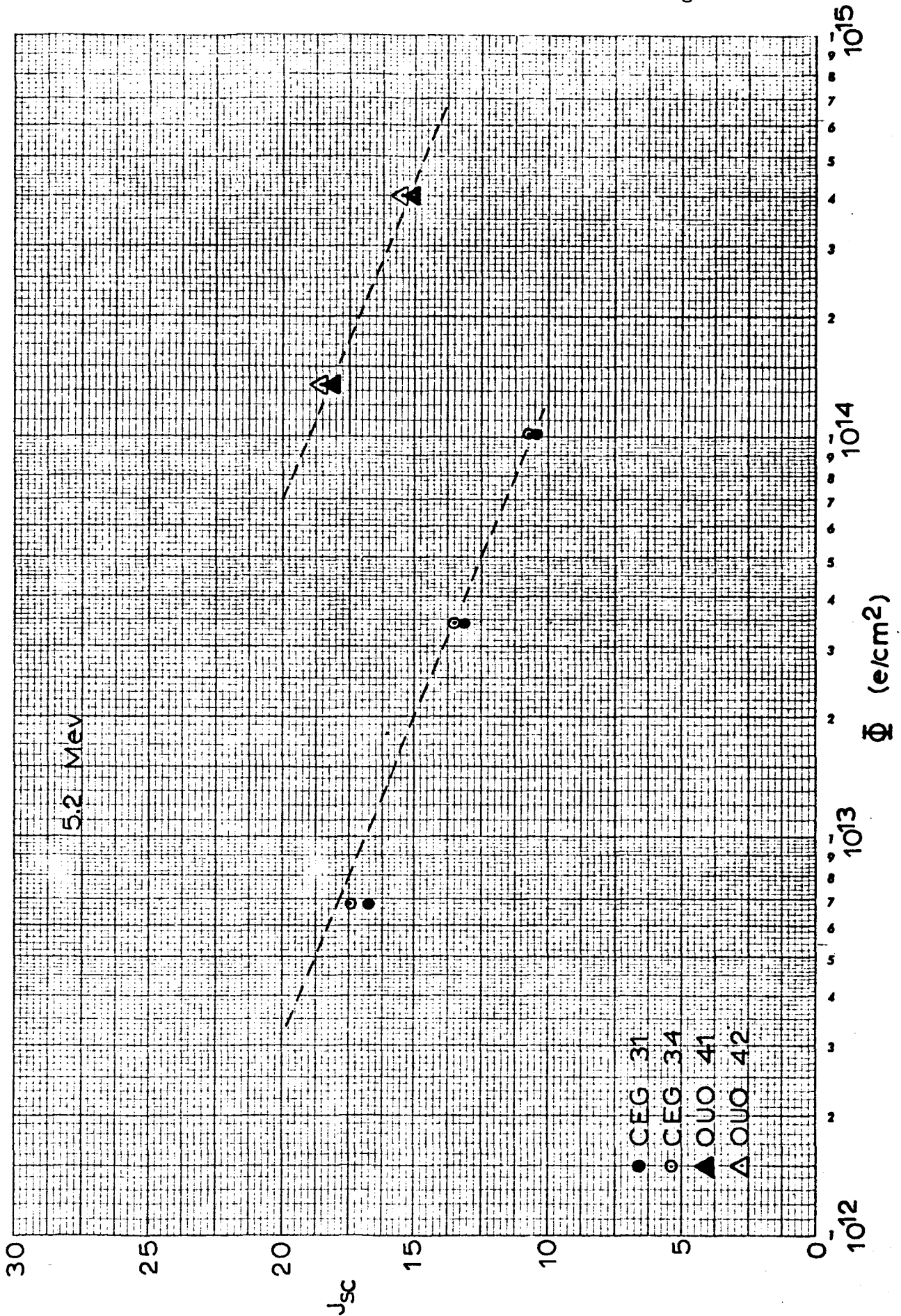


Figure 2. Solar Cell Short Circuit Current Degradation Under 5.2 Mev Electron Bombardment

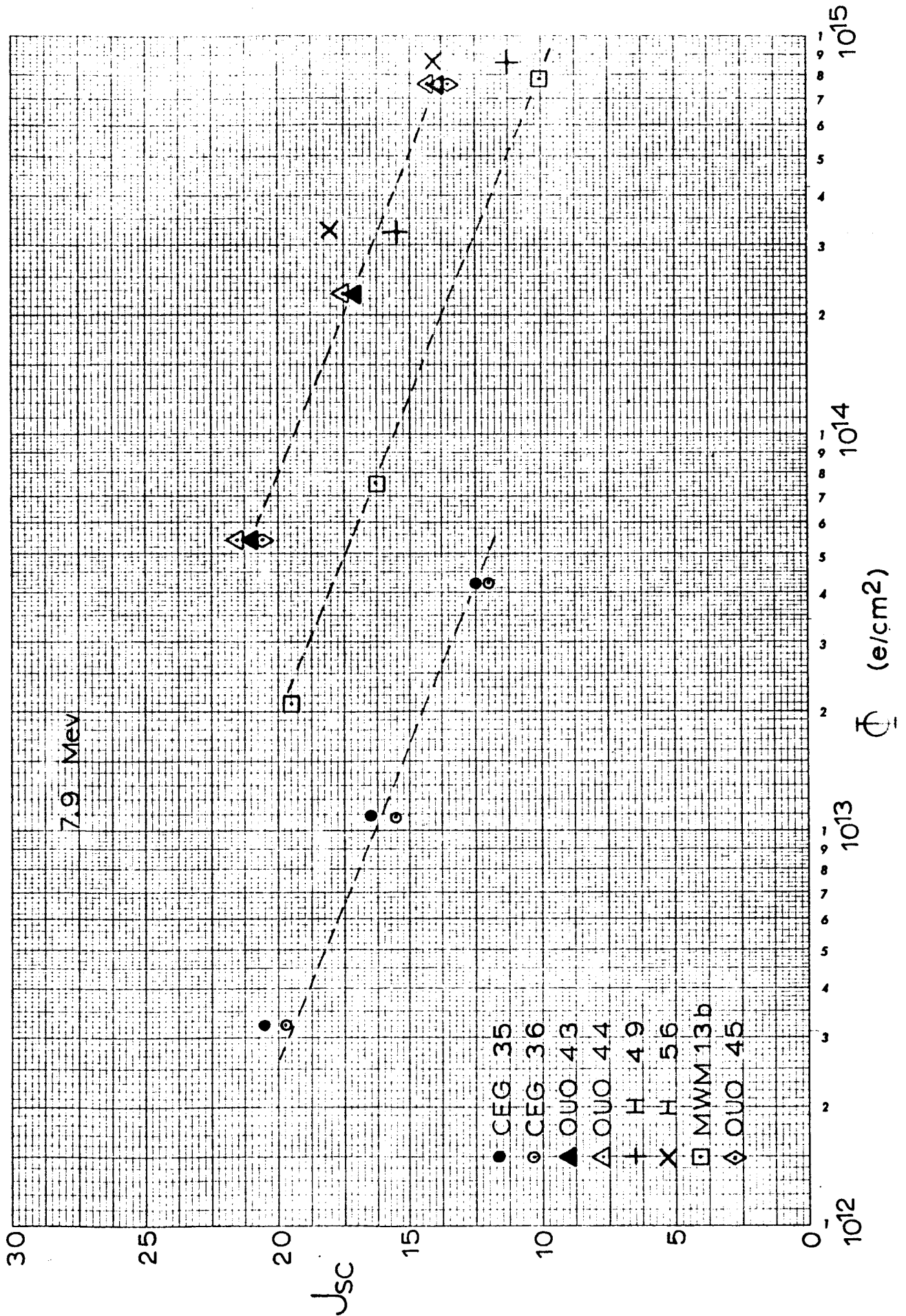


Figure 3. Solar Cell Short Circuit Current Degradation Under 7.9 Mev Electron Bombardment



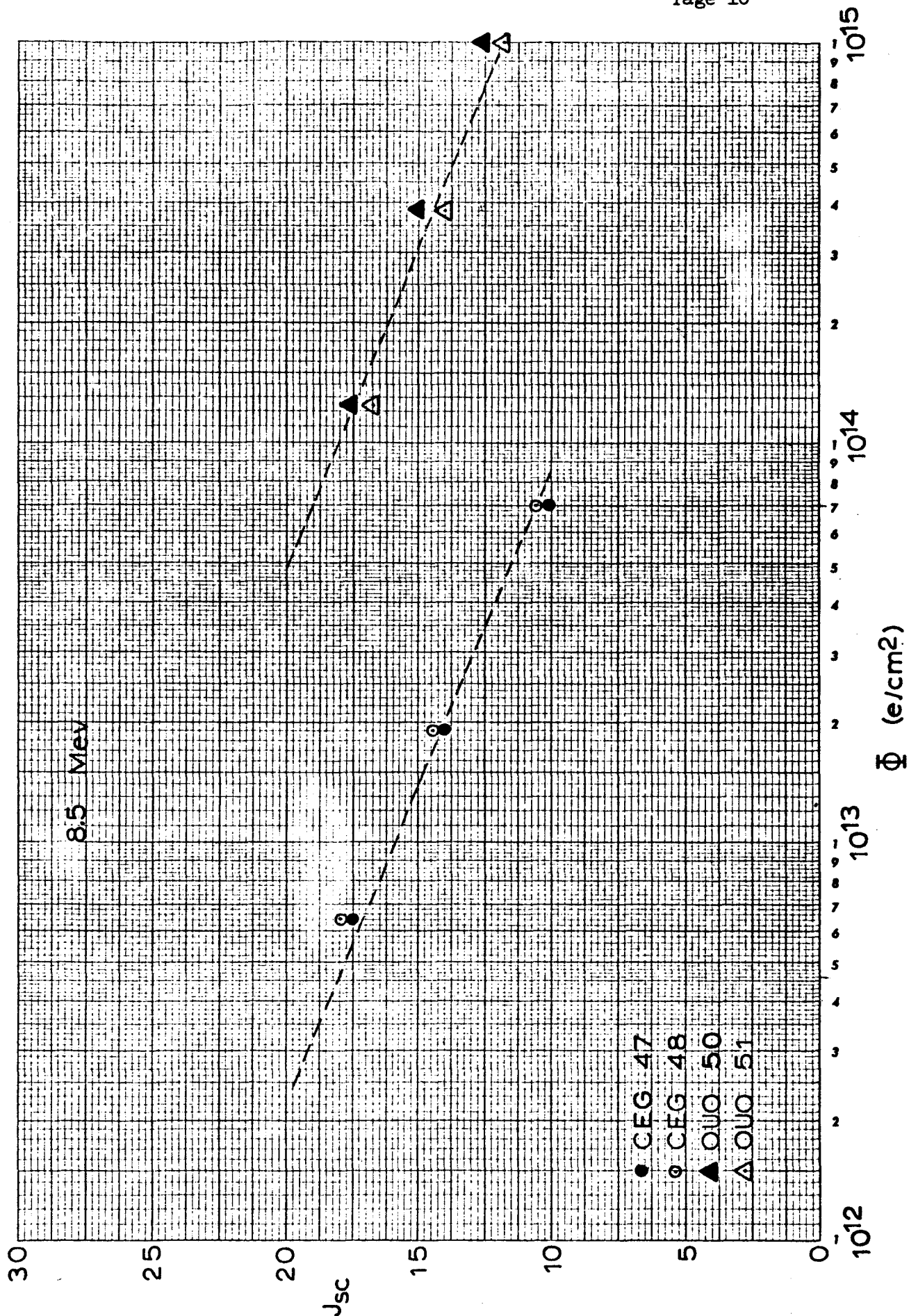


Figure 4. Solar Cell Short Circuit Current Degradation Under 8.5 Mev Electron Bombardment



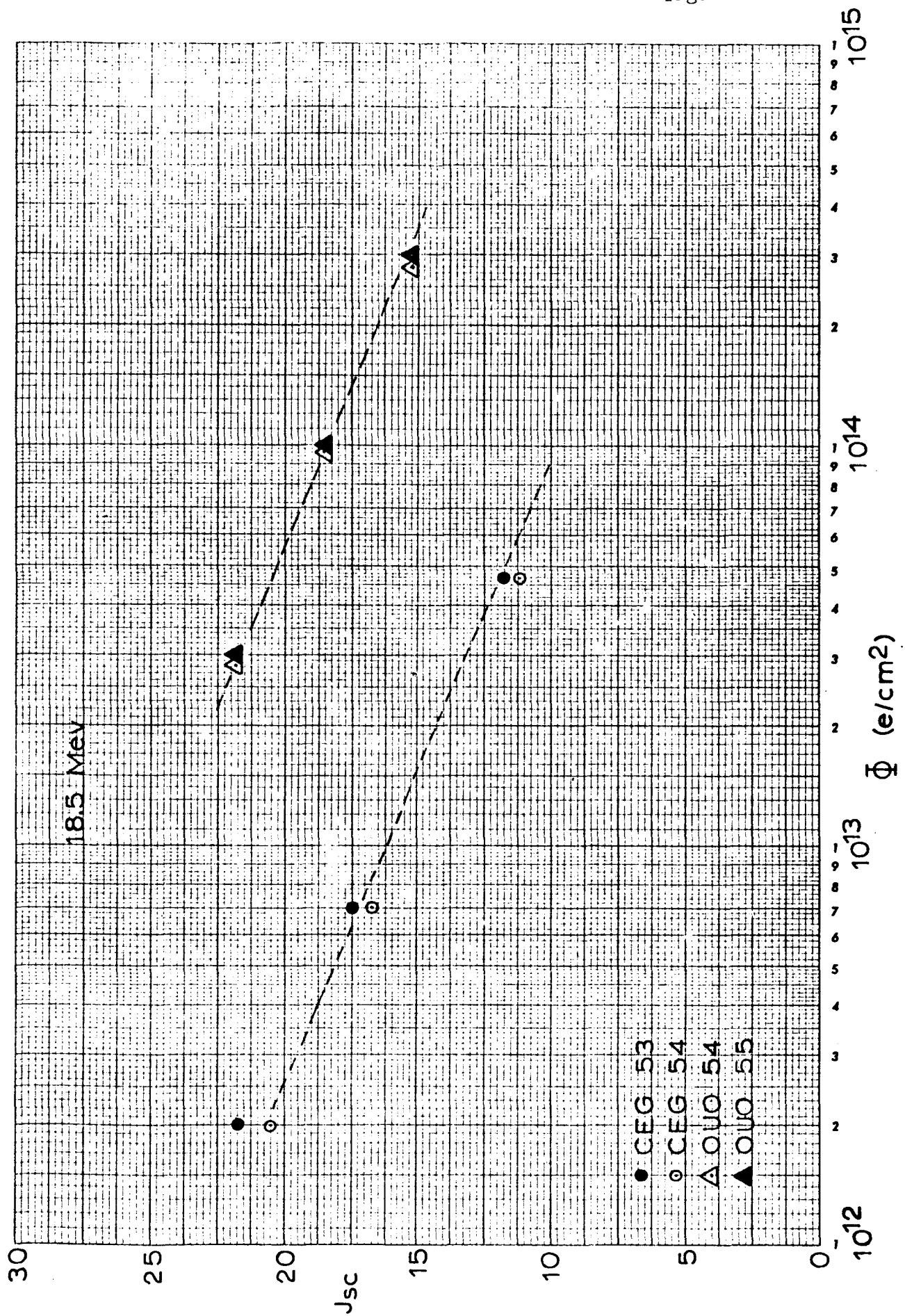


Figure 5. Solar Cell Short Circuit Current Degradation Under 18.5 Mev Electron Bombardment

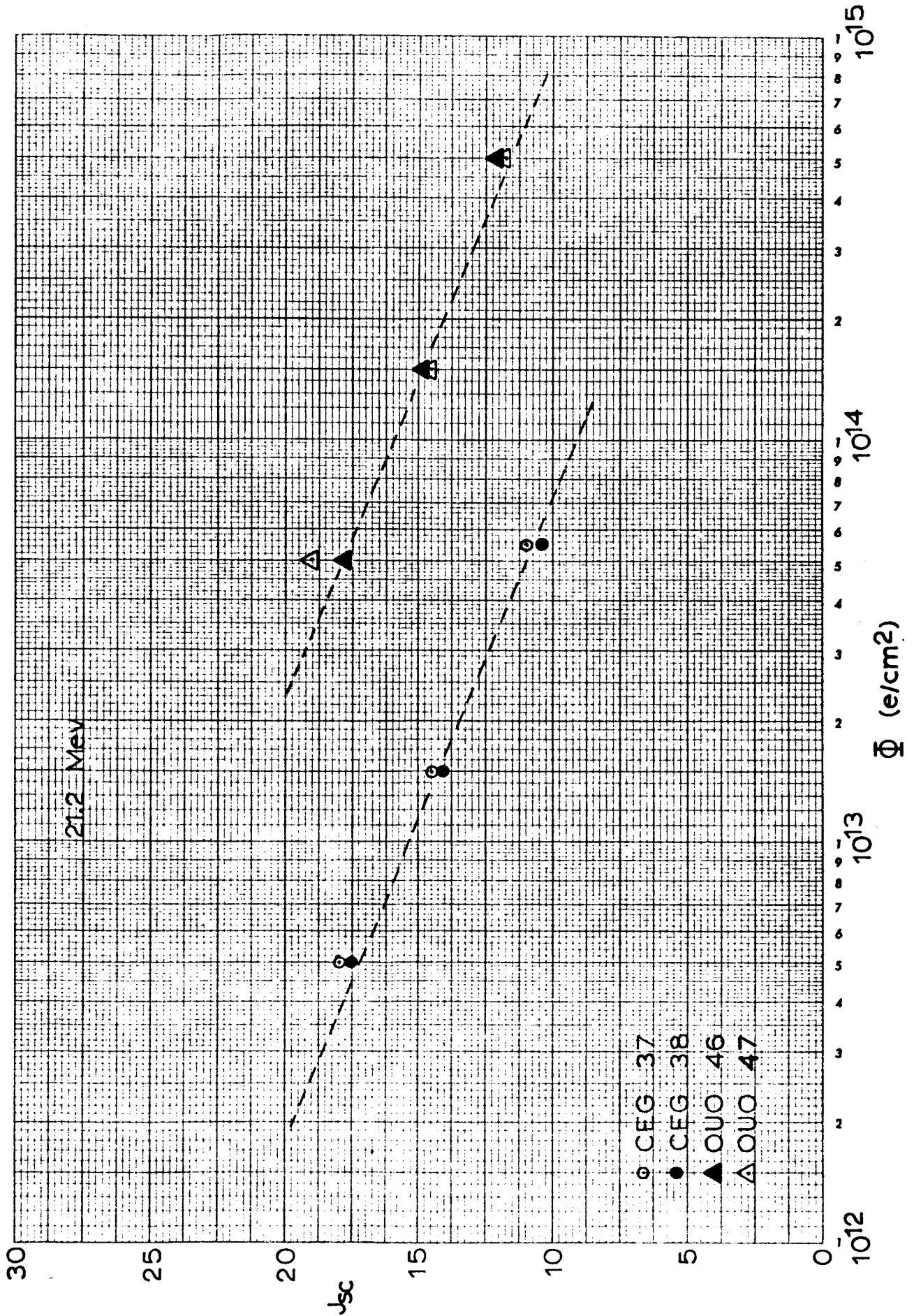


Figure 6. Solar Cell Short Circuit Current Degradation Under 21.2 Mev Electron Bombardment

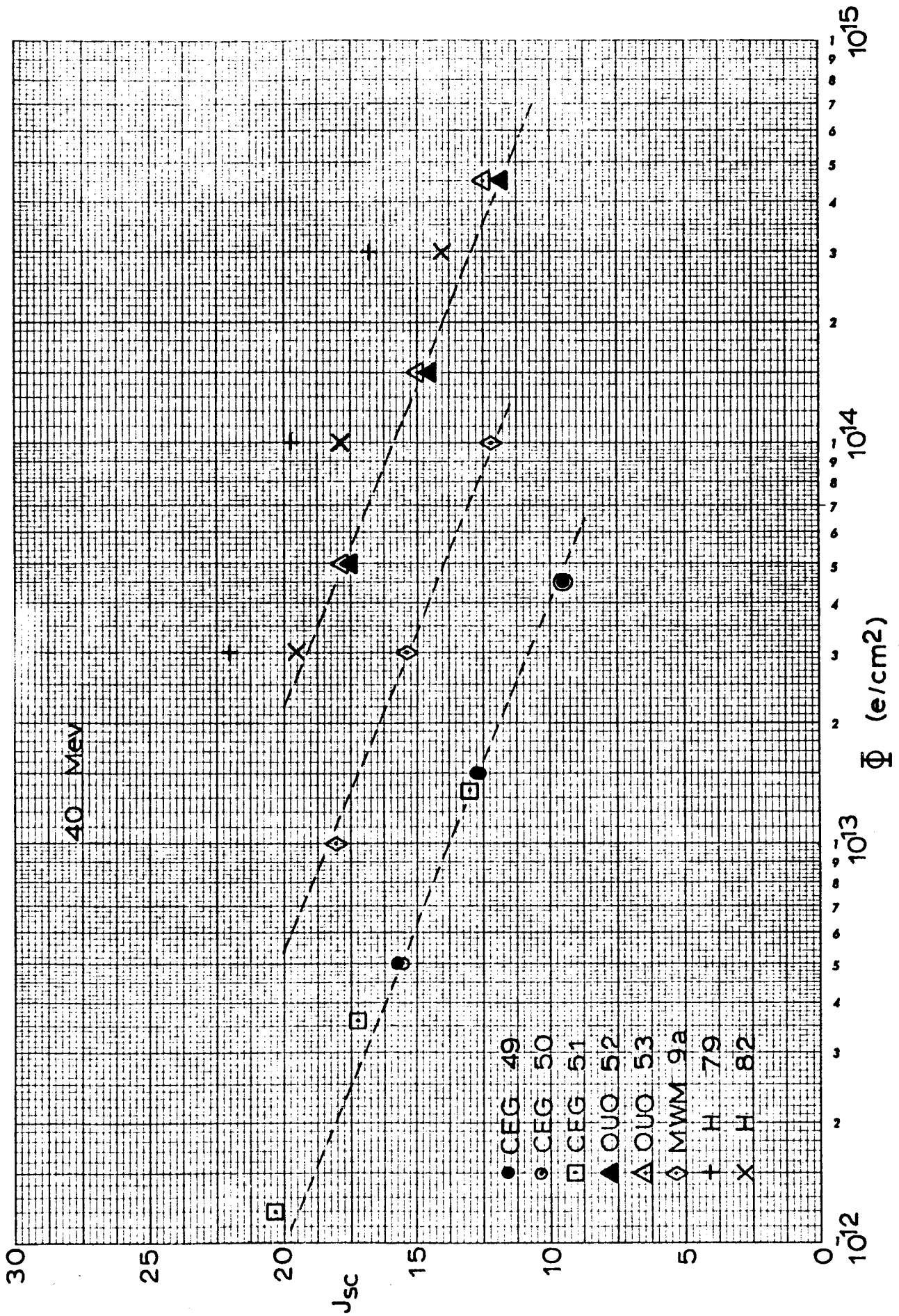


Figure 7. Solar Cell Short Circuit Current Degradation Under 40 Mev Electron Bombardment

diffusion lengths than observed several years ago when this standard was established, current initial short circuit currents are somewhat higher and the per cent of degradation at  $19 \text{ ma/cm}^2$  is usually greater than 25 per cent. However, in order to compare current data with earlier data it is necessary to maintain this level of irradiation damage as a critical flux determination since the resulting minority carrier diffusion lengths in the two cases would then be equal. Gallium arsenide cells, however, exhibit a different characteristic slope because of their difference in optical absorption characteristics. The degradation slope for gallium arsenide solar cells is observed to lie between 45 and 50 per cent degradation in short circuit current per decade of integrated flux for either tungsten or sun illumination. Hence, comparison with silicon cells is difficult since the curves will eventually cross one another although the gallium arsenide cells are initially more radiation resistant. In order to maintain consistency in determining the energy dependence, however, critical fluxes were assigned at 25 per cent degradation for the gallium arsenide solar cells also.

Examination of the short circuit current degradation data in Figures 1 through 7 illustrates that in most cases the data are in good agreement with the expected degradation slope of  $6\text{-}1/4 \text{ ma/cm}^2$  per decade. On several occasions, however, the data do not accurately fit this slope. This deviation from expected slope in these isolated cases is due primarily to shifting accelerator characteristics resulting in corresponding shifts in beam energy and distribution, and hence deviations from the calibrated relationship between integrated flux and monitored Faraday cup current. Since the data were continuously plotted during the course of the experiment, these deviations from normal responses were immediately observed and machine operating characteristic checks such as measurement of beam energy and Polaroid film pictures of beam position were initiated. In all cases of apparent nonlinear response, these performance checks indicated significant machine drift in operating characteristic. At this time the accelerator was retuned to obtain the initial beam characteristics for the experiment before further irradiations were performed. Several portions of the resulting data, therefore, were omitted in the repeated experiments. However, when the deviations were slight in the early stages of accelerator drift, the data are included in an effort to obtain the best possible statistical energy dependence characteristic.

The energy dependence was determined using both reciprocal fluxes and K values. The reciprocal fluxes taken from Figures 1 through 7 are plotted as a function of energy in Figure 8. The 1.0 Mev electron damage characteristics shown in Figure 8 were taken from a previous report<sup>1</sup>. Reciprocal critical fluxes are chosen as the dependent variable since this parameter is proportional to the defect density introduction rate in a manner similar to K values. Examination of Figure 8 clearly illustrates that the energy dependence data describe a smooth curve, with the exception of a few points. The theoretically predicted energy dependence based on Coulomb scattering and simple displacement theory, as outlined in Seitz and Koehler<sup>5</sup>, is shown in Figure 8 as solid lines for comparison with the experimental data shown as dashed lines. The results of the experiment indicate agreement with the previous experiment<sup>3</sup> in that p on n silicon solar cells exhibit an energy dependence in qualitative agreement with theory, whereas both 1 ohm-cm and 10 ohm-cm n on p silicon solar cells depart radically from theory. It is additionally observed that gallium arsenide solar cells respond in qualitative agreement with the theoretically predicted energy dependence although the theory is not directly applicable as presented here to gallium arsenide. In any event, gallium arsenide solar cells do not exhibit a steep energy dependence as do the n on p silicon solar cells.

The departure of the n on p solar cells from theory is quite pronounced. Based on extrapolation of the theoretical predictions from 1 Mev, the damage rate at 10 Mev for n on p silicon solar cells is approximately a factor of 10 higher than the prediction. The importance of this effect will be discussed in greater detail in a following section.

In addition to the energy dependence determined on the basis of reciprocal critical fluxes, measurement of minority carrier diffusion length at both high and low injection levels provides K values which are plotted as a function of energy as shown in Figure 9. The trends shown in Figure 9 are identical with those shown in Figure 8 with only a slight relative displacement of the 10 ohm-cm n on p cells due to their somewhat higher surface efficiency. The gallium arsenide solar cells are not shown in this figure since diffusion length measurements were not obtained on these specimens. Measurements of diffusion length on silicon solar cells at low injection levels with the Van de Graaff accelerator and at high injection levels using the calibrated light source

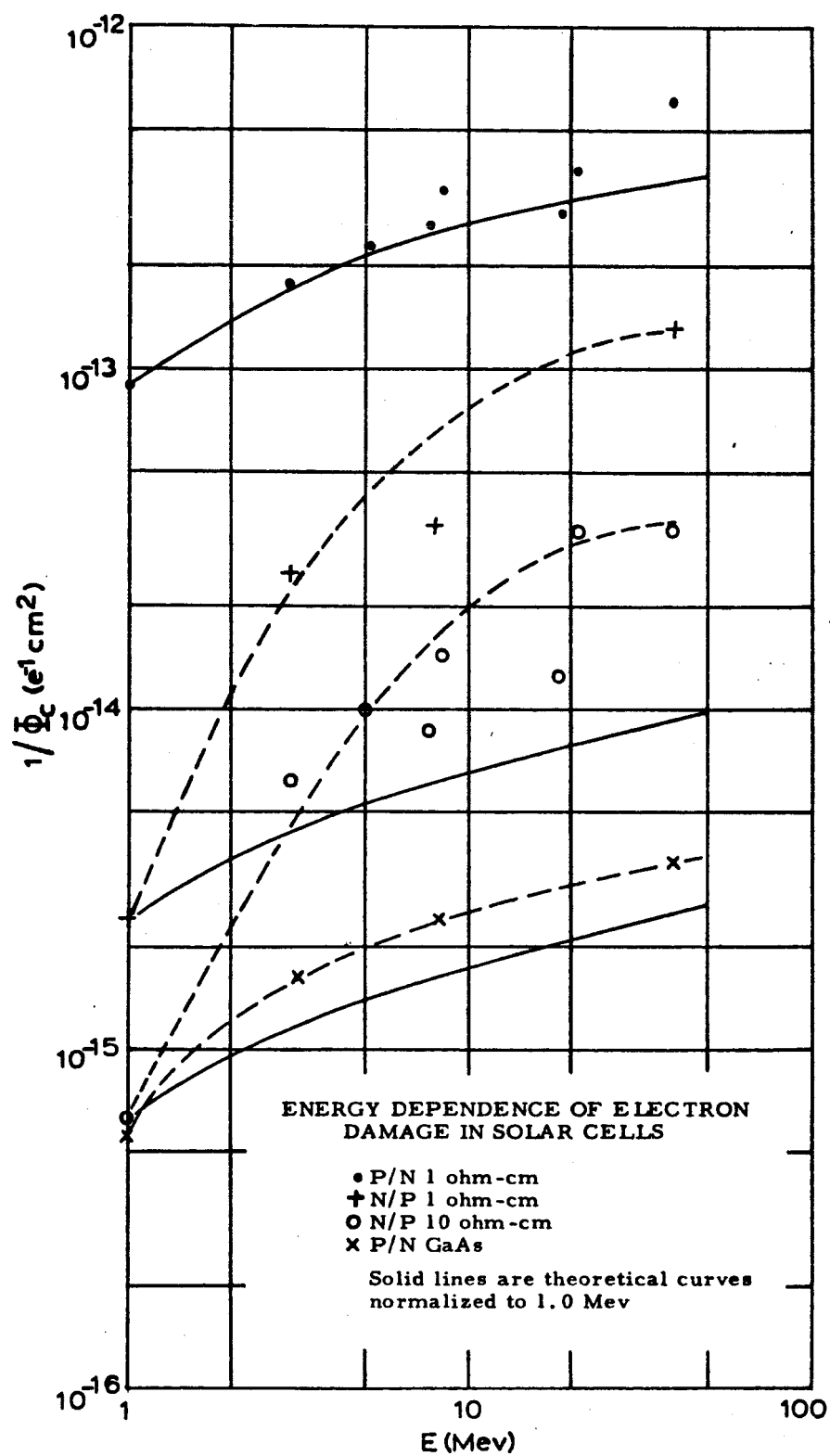


Figure 8. Critical Flux Determination of Electron Damage Energy Dependence

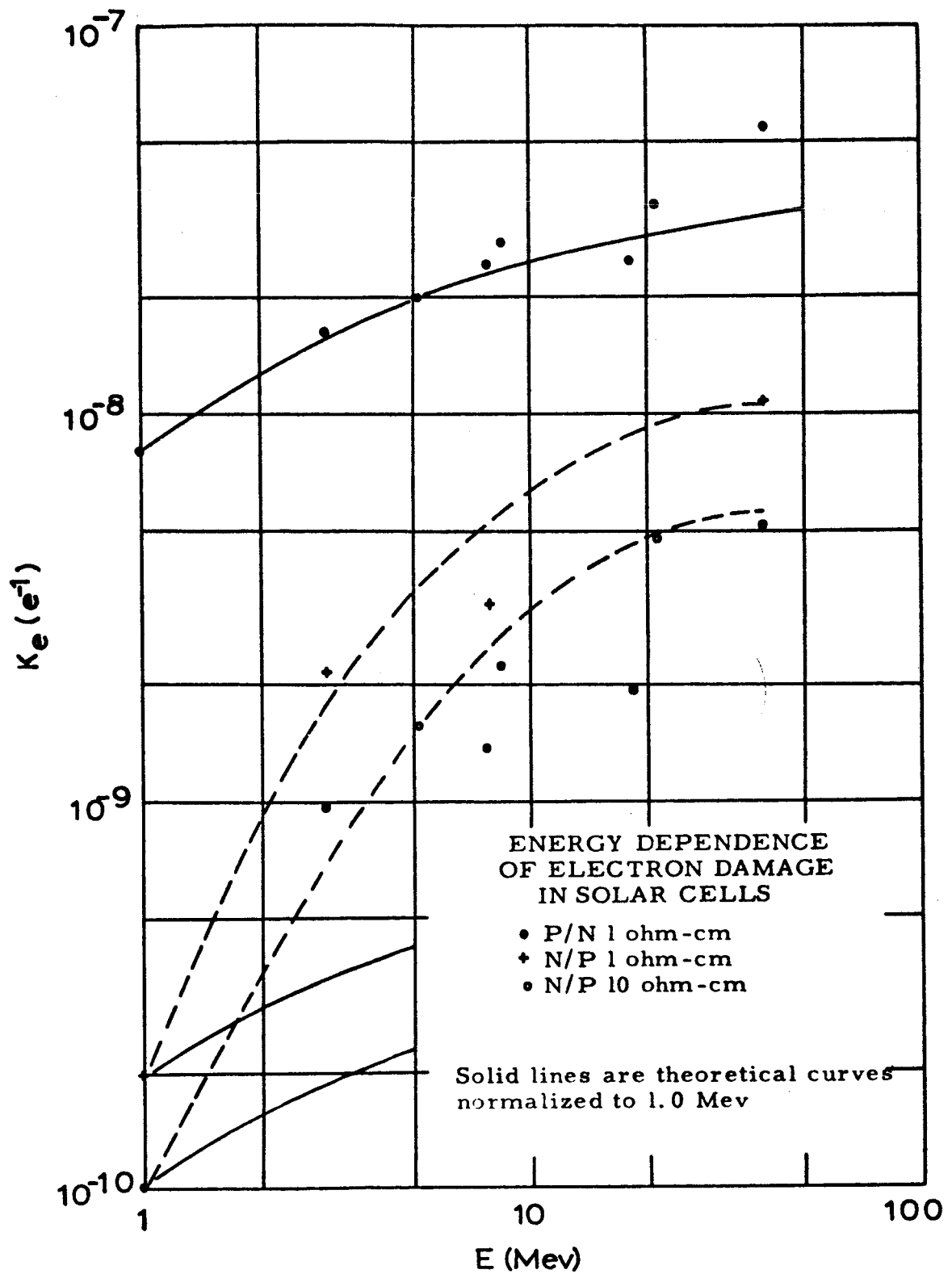


Figure 9. K Value Determination of Electron  
Damage Energy Dependence

yield the same diffusion lengths. Additional measurements were performed to insure that injection level dependence of minority carrier diffusion length was not present in this range in contrast to those data previously reported for proton bombarded silicon solar cells.

The Hall specimens that were irradiated in this experiment were subsequently measured after return to the STL facilities. These data, since not directly pertinent to the energy dependence, are not reported here but are included in an earlier report covering a series of energy level studies under electron and proton bombardment<sup>6</sup>.

#### IV. SUMMARY AND CONCLUSIONS

The primary objective of this experiment was to confirm quantitatively results obtained in an earlier experiment indicating departure of n on p silicon solar cells from theory in their damage dependence on electron energy. The results presented in the previous section have quantitatively established this relationship. N on p silicon solar cells exhibit a much greater dependence of damage rate on electron energy than predicted by theoretical relationships. P on n silicon solar cells and gallium arsenide solar cells exhibit an energy dependence in qualitative agreement with theoretical relationships. The departure of n on p silicon solar cells from the theoretical relationships is approximately an order of magnitude at 10 Mev based on theoretical extrapolation of 1 Mev experimental data. In other words, n on p silicon solar cells are an order of magnitude more sensitive to 10 Mev electrons relative to 1 Mev electrons than p on n silicon solar cells or gallium arsenide solar cells.

The practical importance of this effect lies in the integration of these energy dependence relationships with the fission beta energy spectrum of the artificial electron radiation belt. The result of the folding of the n on p silicon solar cell energy dependence with the artificial belt's energy spectrum is an increase in the predicted damage rate of a factor of three over that predicted on the basis of the energy dependence characteristic of p on n silicon solar cells. This fact reduces by a factor of three the radiation resistance of n on p cells relative to p on n cells considered for spacecraft applications requiring orbit through the artificial radiation belt.



The reasons for the departure of p-type silicon from simple displacement theory in its response to electron radiation are not clear at this time. Since both p-type and n-type silicon are chemically extremely pure silicon, the initial radiation induced interaction is the displacement of silicon atoms from their lattice sites in both cases. The observed peculiar response of p-type silicon under electron bombardment, therefore, must be associated with complex interactions of these defects with other impurities or with each other in a manner not governed by the same energy dependent relationships ascribed to the production of the initial defects.

One particular type of defect which has been hypothesized by many workers in this field and which may be responsible for the interactions observed here is the divacancy. The theoretical relationships governing the energy dependence of the production rate of divacancies have not been formulated. In any event, considerable research remains to be performed on these phenomena before a complete understanding of the effect can be obtained.

## REFERENCES

1. J. M. Denney, R. G. Downing, W. I. Hoffnung, W. K. Van Atta, Charged Particle Radiation Damage in Semiconductors, V: Effect of 1 Mev Electron Bombardment on Solar Cells, Contract No. NAS5-1851, dated 11 February 1963.
2. William R. Cherry and Luther W. Slifer, Solar Cell Radiation Damage Studies with 1 Mev Electrons and 4.6 Mev Protons, NASA, Goddard Space Flight Center, Greenbelt, Maryland, dated 27 May 1963.
3. J. M. Denney, R. G. Downing, G. W. Simon, W. K. Van Atta, Charged Particle Radiation Damage in Semiconductors, VI: The Electron Energy Dependence of Radiation Damage in Silicon Solar Cells, Contract No. NAS5-1851, dated 13 February 1963.
4. J. M. Denney, R. G. Downing, M. E. Kirkpatrick, G. W. Simon, W. K. Van Atta, Charged Particle Radiation Damage in Semiconductors, IV: High Energy Proton Radiation Damage in Solar Cells, dated 20 January 1963.
5. Frederick Seitz and J. S. Koehler, Solid State Physics, 305, 2, (1956).
6. J. R. Carter, Jr., R. G. Downing, Charged Particle Radiation Damage in Semiconductors, VII: Energy Levels of Defect Centers in Electron and Proton Bombarded Silicon, Contract No. NAS5-1851, dated 15 February 1963.